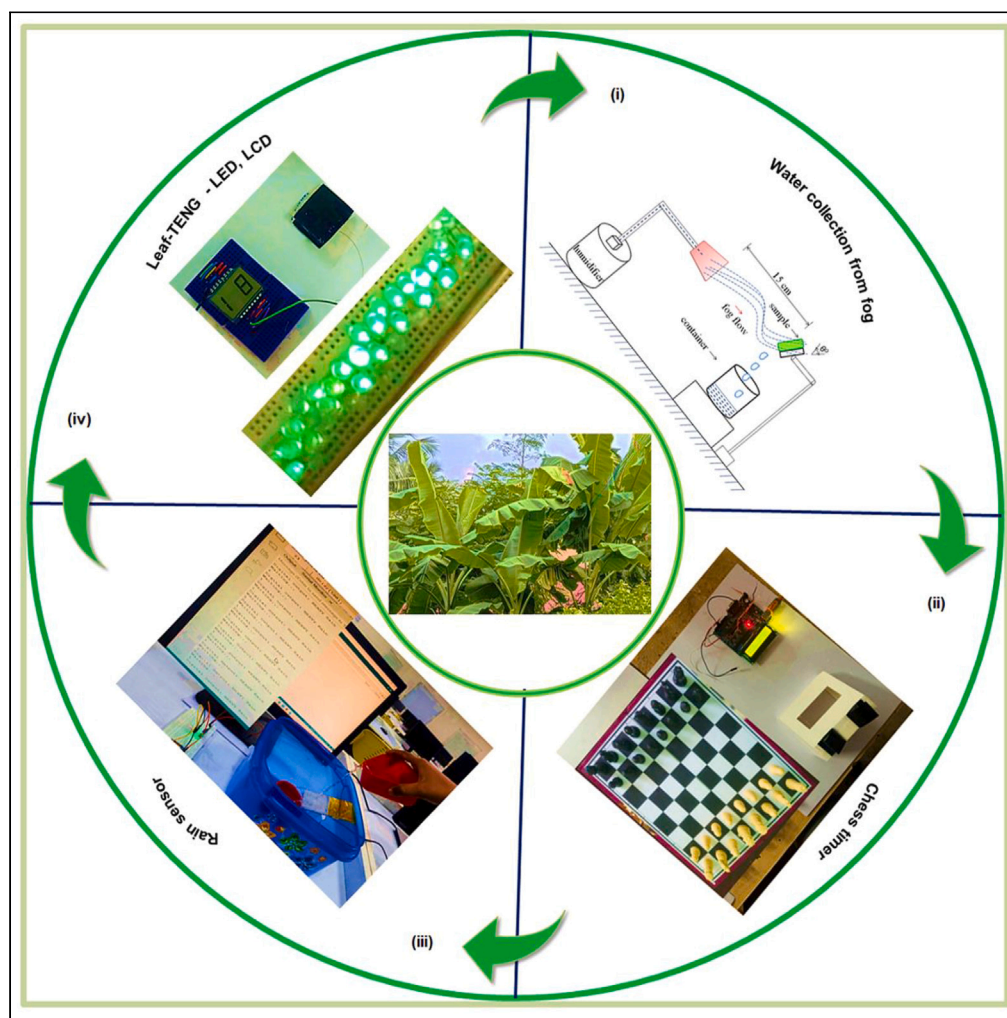**Article**

Biomimicking hydrophobic leaf structure using soft lithography for fog harvesting, triboelectric nanogenerators as a self-powered rain sensor

Shaik Ruksana
Begum,
Arunkumar
Chandrasekhar

arunkumar.c@vit.ac.in

Highlights

Ecoflex patterns made with molds and lithography

The profilometer and goniometer measure leaf roughness

Leaf patterns enhance nanogenerator and fog capture

Leaf-TENG chess clocks combine theory and real life

Article

Biomimicking hydrophobic leaf structure using soft lithography for fog harvesting, triboelectric nanogenerators as a self-powered rain sensor

Shaik Ruksana Begum[1] and Arunkumar Chandrasekhar[1,2,*]

SUMMARY

This study focused on the soft lithography technique of transferring the shape of a leaf's surface using a polymer film made by replicating the different patterns on the surfaces of four leaves. These films were used to collect fog water and to create TENGs for self-powered rain sensors. This research mainly focuses on analyzing the potential surface patterns of leaf films to improve fog water collection, enhancing the efficiency of TENGs, and looking at freshwater shortages in arid areas. The evaluations included surface morphology, contact angles, and structural analysis with goniometric drop morphology and 3D optical profilometry. Leaf-based TENGs showed promising power density, stability, and charging for energy gathering. Furthermore, the TENG devices showed their ability to detect raindrop patterns, highlighting their potential uses in promoting environmental sustainability. Hence, the result revealed that biomimicry can produce eco-friendly energy harvesting and sensor systems to reduce water scarcity and advance renewable energy.

INTRODUCTION

Due to the growing need for green energy, sustainable energy from the environment is a prevalent study issue for energy crisis management. Renewable energy sources like wind, solar, and water have made these developments feasible. It has led to the development of renewable energy conversion technologies, including wind turbines, tidal power generators, and solar cells.[1–3] The need for clean and sustainable energy worldwide has led to the creation of new technologies and tools for converting energy. These developments allow for the effective use of renewable energy sources, which helps protect the environment, increase energy security, and promote economic growth. The triboelectric nanogenerator (TENG) is an emerging technology that converts mechanical energy into electrical energy by combining electrostatic induction and triboelectric electrification. TENG provides significant advantages due to its lightweight, high energy conversion efficiency, low cost, and adaptability to various types of energy.[4] The TENG uses frictional energy from the environment, which is everywhere. TENG can capture and convert frictional mechanical motion into electricity, making it a versatile energy source. Examples are mechanical motion,[5] ocean waves,[6] rainfall,[7] wind,[8] friction,[9] and motion energy.[10] It has several industry and sector applications that can power self-sustaining detection and sensing equipment,[11,12] provide lighting,[13] and drive self-powered electrochemical oxidation systems,[14,15] among many other things, to solve energy and environmental issues.

TENG devices' real-world electrical output frequently needs to improve their theoretical capabilities. Real-world issues, including material constraints, environmental considerations, and energy conversion losses, all contribute to this difference.[16,17] Various factors influence the effectiveness of TENG devices, such as the choice of triboelectric materials,[18] the design of the structure,[19] the working surroundings,[20] and proper material property analysis, and contact interface design optimization, which are essential for enhancing the consistency of friction-induced motion.[21] Previous work has demonstrated that increasing the surface roughness of triboelectric materials can significantly improve the electrical performance of TENG devices.[22] TENG devices can also be self-powered sensors for vibration, speed, and human motion tracking without extra power supply equipment.[23–25] This self-sufficiency makes TENG devices highly desirable for various sensing applications, such as wearable technology,[26] structural health monitoring,[27] and environmental sensing.[28] Currently, the efforts of researchers have resulted in an increase in the structural design of TENG devices based on harvesting mechanical energy. Many materials, such as inorganic metals and thin-film biological materials, can be triboelectric materials.[29–31]

Surface micro/nanomanufacturing techniques are essential in many areas, such as microelectromechanical systems (MEMS),[32] microelectronics,[33] optical MEMS,[34] and microfluidics/lab-on-a-chip.[35] Many recent studies looked into the possibilities of soft lithography for

[1]Nanosensor and Nanoenergy Lab, Department of Sensor and Biomedical Technology, School of Electronics Engineering, Vellore Institute of Technology, Vellore, Tamil Nadu 632014, India
[2]Lead contact
*Correspondence: arunkumar.c@vit.ac.in

employing natural templates as main molds to create or replicate structures.[36] Researchers examined the impact of various leaf surface characteristics, including stomata, epidermal wax, and trichomes, on contact angle measurements.[37] Several research studies have proposed a low-cost replication technology that utilizes wax crystals to cover each natural and artificial surface to achieve exceptional resolution.[38] An independent research undertaking compared the wettability of three hydrophobic plant leaves with that of an aluminum alloy using biomimetic replication of a superhydrophobic surface.[39] In addition, various studies were conducted to analyze the topography and wettability of the lower surfaces of English weed (Oxalis escape) leaves, along with their reproduced biological equivalents.[40] Lithography methods enable the creation and replication of micro- and nanoscale structures, allowing for fine-grained control of surface features. The technique is known as soft because it uses flexible materials like the Ecoflex polymer. Researchers use soft lithography to develop distinctive characteristics and non-wetting qualities in molds inspired by nature, to roughen the working materials and increase the efficiency of TENGs.[41,42] To manufacture surfaces with suitable roughness qualities, researchers have been actively experimenting with combining soft lithography and primitive plant patterns.[43]

This research aimed to assess and improve the functionality of soft lithography-generated surfaces. Ecoflex was selected as a silicone elastomer due to its incredible ability to mimic the characteristics of plant leaves. The unique features of leaves are replicated by taking pictures of their surfaces and then correctly reproducing them on an Ecoflex polymer substrate. The roughnesses of the leaf surfaces are measured using goniometric drop morphology and a 3D optical profilometer. Goniometric drop morphology is depositing a droplet of liquid (for example, water) on the leaf surface and measuring the contact angle, which can provide information about the surface's hydrophobicity or hydrophilicity. Also, the surface morphology and structure of the polymer film are studied using a 3D optical profilometer at 1000x magnification. These leaf films also fabricate Leaf-TENG devices used as touch-sensitive switches in chess timing systems, showing their interactive potential. The Leaf-TENG was evaluated with four distinct Ecoflex leaf roughnesses in the experiments. Compared to the other three leaves' roughnesses, the banana roughness performed the best, with open-circuit voltage (V_{oc}) and short-circuit current (I_{sc}) values of 78.5 V and 17.5 µA, respectively. Also, when the Leaf-TENG was combined with leaf-shaped films, it collected a power density of 2.43 µW/cm^2. The leaf surface patterns enable TENGs to work better while also showing potential in the collection of fog water, solving the problems of both energy and water scarcity.

Furthermore, this study investigates the operation of rain-sensing TENG devices with single electrodes and freestanding triboelectric layer modes. TENG devices for rain detection are essential since they utilize the triboelectric effect to convert the mechanical energy from rainfall into electrical energy, making rain detection TENG devices particularly captivating. Thus, this research advances TENG technology for energy harvesting, touch sensing, and rain-sensing applications.

RESULTS AND DISCUSSION

Methods and materials

Leaf selection and preparation

Based on their micron-scale visible surface patterns, four different leaves were selected for this study: arrowhead, Sanchezia, banana, and money plant. Figure 1 shows the wettability, the presence of a waxy epicuticular layer, and the shape and size of their surface microstructures. The surface wettability of the selected leaves ranged from hydrophilic to superhydrophobic. The leaves are collected from the plants and used within 30 min to prevent excessive dehydration. Before use, the top surfaces of the leaves were carefully washed with purified water to remove any dirt particles during the sampling process, keeping away the leaf's primary veins or vascular systems to protect the mold surface as much as possible.

Figure 1A presents a schematic flowchart for producing a micro-patterned Ecoflex fabrication process using a money plant leaf as the mold. The mesophyll-embedded venation, which provides mechanical stability and other valuable properties, is primarily responsible for the leaf's rich textures. Cut the leaf to the right shape and affix it to the bottom of the die, as shown in Figures 1B and 1C. After preparing the leaf mold, the Ecoflex base and crosslinker were added, as shown in Figure 1D: Clean the edge of the mold well to remove any dust or dirt that could stop the Ecoflex material from sticking. Mix the Ecoflex and crosslinker according to the manufacturer's instructions. It is essential to achieve the required mechanical properties. Mix the Ecoflex and crosslinker thoroughly to obtain consistent consistency. Inadequate mixing may cause uneven curing and mold adherence. Use a spatula or another suitable tool to spread the Ecoflex mixture on the edge of the mold. Make sure the material is evenly distributed over the whole area. After applying Ecoflex:

(1) Press it gently against the mold to ensure suitable contact.
(2) Pay special attention to areas that may contain confined air bubbles.
(3) Use a roller or something else like it to eliminate any bubbles.

As shown in Figure 1E, the prepared Ecoflex solution is poured evenly on the entire leaf sheet and kept to dry on a flat surface, left to cure on a hot air drier for 10 min at 60°C to set and take the form of the mold. After fixing the solution, look at it to ensure it has stuck evenly to the mold surface. Investigate any uneven spots or areas where the material has not adequately conformed. Test the cured Ecoflex to ensure it keeps its flexibility and securely attaches to the mold. We can look for any indications of delamination by gently pressing on the material or giving it some movement. To check for delamination, gently squeeze or flex the material. The cured film is then peeled off from the leaf sheet to obtain a roughness-created Ecoflex film, and the visual representation of the leaf surfaces provided by the real-life images aids in comprehending their macroscopic appearance and texture in Figure 1F. This approach offers a simple, cheap, and ecologically friendly way of creating molds with accurate micro textures. Also, this procedure can be extended to other leaves, and a similar process can be used to make different mold patterns.
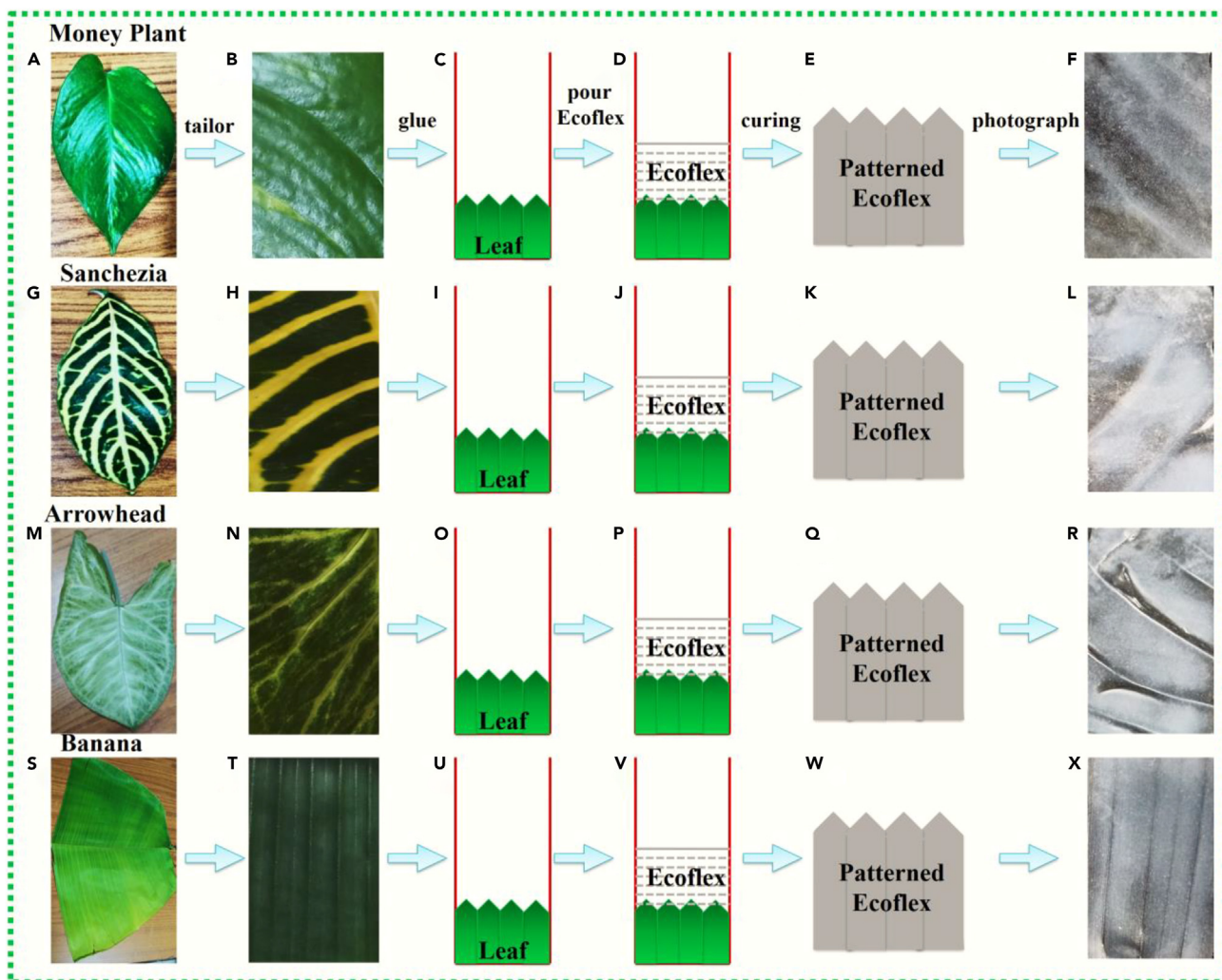
Figure 1. Plant leaves and Ecoflex manufacturing process

(A) Money Plant leaf used as a prototype mold.

(B) Proper slicing of the leaf into the desired form.

(C) Leaf entrapped in the die.

(D) Ecoflex coating applied to the leaf.

(E) Flexible Ecoflex mold.

(F) Image of Ecoflex film with elastic microstructure.

(G–L) Schematic flow diagram for Sanchezia leaf-patterned Ecoflex fabrication.

(M–R) Schematic flow diagram for Arrowhead leaf-patterned Ecoflex fabrication.

(S–X) Schematic flow diagram for Banana leaf-patterned Ecoflex fabrication.

In this study, soft lithography was successfully employed to transfer the surface patterns of the chosen leaves onto cleaned surfaces using a silicon elastomer with an Ecoflex base, as shown in Figure S1 in supporting information. The leaf was cut into (3 × 3 cm) pieces and pasted onto an acrylic sheet to create a mold. It generated a homogeneous polymer solution after carefully combining parts A (23g) and B (23g) of the Ecoflex elastomer for 15 min. The solution was then evenly applied to the entire leaf sheet, which was then allowed to air dry for about an hour on a flat surface. The polymer solution, drying and taking on the leaf's shape and texture, formed an irregular pattern on the film. After curing, the film peeled away from the leaf, leaving the Ecoflex film with the desired roughness and leaf design.

Evaluation of the mold surface

Optical microscope analysis. The molds of four various leaf patterns (money plant, Sanchezia, arrowhead, and banana) were examined under an optical microscope to compare and contrast the roughness of their surfaces Figures 2A1–2A4 and make leaf microfeatures simpler
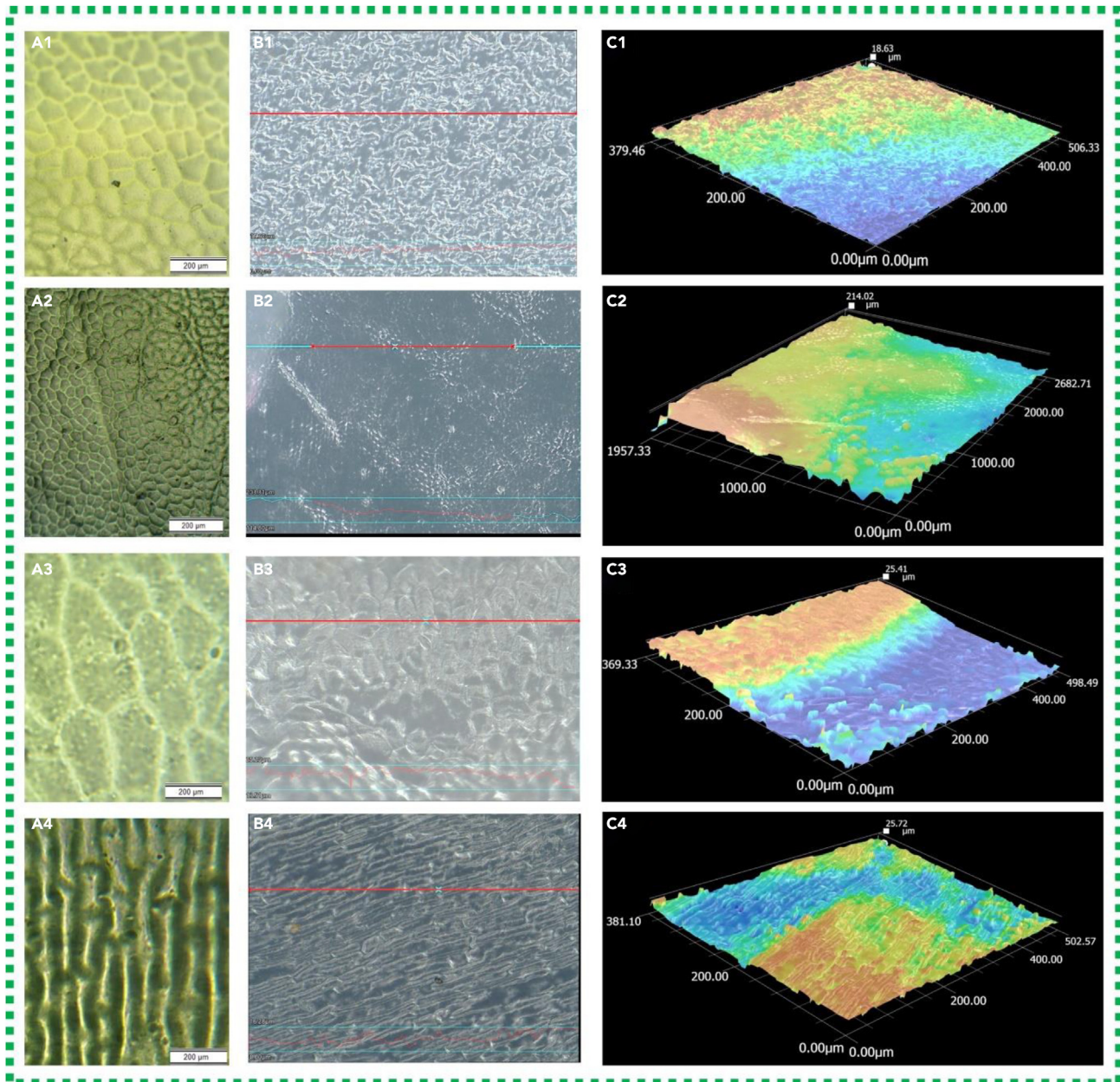
Figure 2. Pictures of the leaf surface roughness were taken using an optical microscope and 3D profilometer

(A1) Money plant.

(A2) Sanchezia.

(A3) Arrowhead.

(A4) Banana.

(B1–B4) Four mages of leaf surface roughness were measured in 3D using an optical surface profilometer.

(C1–C4) Four photographs of the same designs at 1000x magnification.

to observe Figure 2. These features affect the entire surface roughness, which varies in texture, shape, and roughness. The microscope pictures show detailed patterns and abnormalities that affect the performance of soft lithography-fabricated triboelectric nanogenerators.

3D optical profilometer analysis. The other analysis for surface roughness is the 3D optical profilometer, which is one of the essential tools for looking at the hardness of leaf surfaces because it lets you look at small surface details without damaging the leaf. This method uses advanced optical techniques to make accurate and thorough measurements without touching the leaf's surface, which protects its integrity.
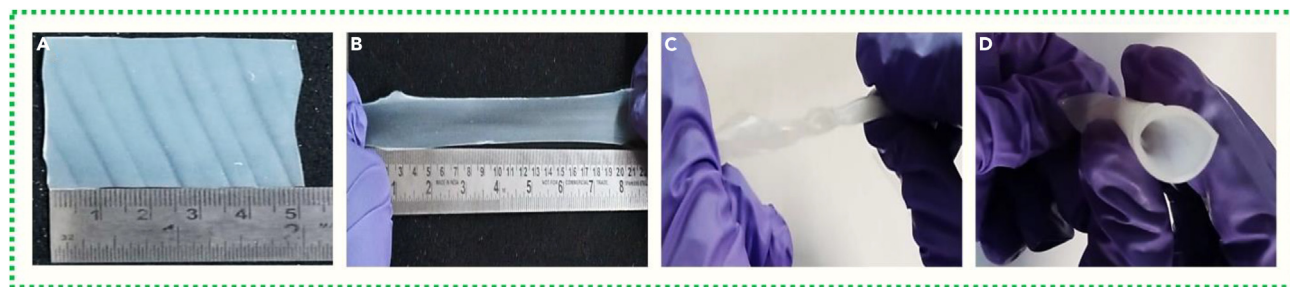
Figure 3. Mechanical properties of Ecoflex leaf patterned films
(A) Normal state.
(B) Stretchability.
(C) Twistability.
(D) Rollability.

The fast scanning speed of the technology makes it possible to quickly gather data from many samples while also making quantitative and standardized measures based on set parameters, like those in ISO standards. This way of doing things gives you a complete picture of surface flaws by showing them in 3D, including the terrain details and the depth of the surface features. This level of detail is beneficial for studying the link between surface roughness and essential leaf functions. It helps us understand plant physiology, how plants adapt to their environment, and how these findings could be used in many scientific fields, such as biomimicry, agriculture, and environmental studies. A 3D optical surface profilometer examined molds with four leaf designs: money plant, Sanchezia, arrowhead, and banana. Figures 2B1–2B4 show the entire study done using this method to determine and measure how rough the surfaces of these leaf pattern molds are. An additional survey result was 3D images showing surface roughness at a 1000x magnification level for each leaf design, as shown in Figures 2C1–2C4. These drawings were very detailed and helped us understand the complex topography that can be found on the surfaces of the different leaf designs.

Goniometric drop morphology analysis. The wetting properties of the replicated mold surfaces were analyzed using goniometric drop morphology. The primary purpose of the goniometric drop method, also called contact angle goniometry, is to measure the contact angle of a liquid drip on a solid surface. It cannot directly measure surface roughness, but it can reveal surface features connected to it.

Figure 3 displays the Ecoflex leaf patterned films' outstanding mechanical capabilities, demonstrating flexibility and durability. The above Figure shows various mechanical situations and material performance. Figure 3A shows Ecoflex's natural flexibility and resilience. Figure 3B shows Ecoflex's stretchability—a stretchable material without compromising structural integrity. Figure 3C shows Ecoflex's twist ability and bending nature. Figure 3D shows Ecoflex's rollability, which is undamaged, and also indicates that the Ecoflex film can be rolled or folded without damage.

Surface structure refers to the physical characteristics and features of the highest layer of a material. It includes the presence of texture, porosity, and micro- or nanoscale features. On the other hand, wettability characterizes a material's attraction to a liquid. At the same time, wettability defines a substance's propensity toward a liquid. The equilibrium between adhesive and cohesive forces at the liquid-solid interface controls it. Due to the larger surface area that is accessible for liquid adhesion, a rougher surface often has a higher tendency to be wettable.

Table 1 compares leaf characteristics and natural surfaces as triboelectric nanogenerators. The table directly compares the output performance and raw materials of TENGs built with these leaves. Thus, the table provides essential information regarding natural materials as effective and sustainable TENG solutions.

Contact angle measurement

Figure S2 shows a 2D cross-section of a water droplet on a solid surface, showing contact angle and wetting. The contact angle is where the droplet's boundary meets the solid surface. The contact angle between the droplet and the surface is a critical characteristic of the droplet's wetting behavior.

In supporting information, three-phase boundary contact angles and interfacial pressures are represented graphically.[47] Applying Young's Equation to a particular solid-liquid system using the three thermodynamic parameters γ_{lv}, γ_{sl}, and γ_{sv} yields a single, system-specific contact angle θ_c.[48] The most significant correlations between the contact angle θ_c, the surface energy of a solid γ_{sv}, the surface tension of a solid γ_{sl}, and the surface tension of a liquid γ_{lv} are given in Equation 1.[49]

$$\mathrm{Cos}\ \theta_c = (\gamma_{sv} - \gamma_{sl}) / \gamma_{lv}$$
(Equation 1)

The relationship between three parameters determines the value of $\cos\theta_c$.

(1) The surface tension between the liquid and solid (γ_{sl})

Table 1. Comparative analysis of various leaves as triboelectric nanogenerator materials

S No	Triboelectric pair material 1	Used mode and fabrication methods	Triboelectric pair material 2	Output performances	Contact area (cm^2)	Mechanical excitation	Reference
1	Hosta leaf	Single-electrode mode & Handmade	(Poly Methyl Meth Acrylate) (PMMA)	V_{oc} = 230 V I_{sc} = 9.5 μA p = 2185 μW $P_{density}$ = 34.1 μW cm^{-2}	8 × 8	2 Hz	Jie et al.[44]
2	Lotus	Single-electrode mode & Handmade	(Poly Methyl Meth Acrylate) (PMMA)	V_{oc} = 100 V I_{sc} = 2.8 μA p = 280 μW $P_{density}$ = 4.4 μW cm^{-2}	8 × 8	2 Hz	Jie et al.[44]
3	Rhododendron leaves	Single-electrode mode & Handmade	Ecoflex (silicone elastomer film)	V_{oc} = 140 V $P_{density}$ = 15 μW cm^{-2}	4.5 × 4.5	10 Hz	Meder et al.[45]
4	Fresh leaf	Contact-separation mode Spin coating & Handmade	(PolyVinyliDene Fluoride) (PVDF)	V_{oc} = 430 V I_{sc} = 15 μA p = 6450 μW $P_{density}$ = 403.1 μW cm^{-2}	4 × 4	5 Hz	Feng et al.[46]
5	E. aureum	Single-electrode mode & Handmade	(Poly Methyl Meth- Acrylate) (PMMA)	V_{oc} = 90 V I_{sc} = 2 μA p = 180 μW $P_{density}$ = 2.8 μW cm^{-2}	8 × 8	2 Hz	Jie et al.[44]
6	Populus	Single-electrode mode & Handmade	(Poly Methyl Meth- Acrylate) (PMMA)	V_{oc} = 115 V I_{sc} = 3.5 μA p = 402.5 μW $P_{density}$ = 6.3 μW cm^{-2}	8 × 8	2 Hz	Jie et al.[44]
7	Firmiana	Single-electrode mode & Handmade	(Poly Methyl Meth- Acrylate) (PMMA)	V_{oc} = 90 V I_{sc} = 2.8 μA p = 252 μW $P_{density}$ = 3.9 μW cm^{-2}	8 × 8	2 Hz	Jie et al.[44]

Table 1. *Continued*

| S No	Triboelectric pair material 1	Used mode and fabrication methods	Triboelectric pair material 2	Output performances	Contact area (cm^2)	Mechanical excitation	Reference
8	Money Plant	Contact-separation mode & Handmade	Ecoflex (silicone elastomer film)	V_{oc} = 17.3 V I_{sc} = 7.5 μA p = 129.75 μW $P_{density}$ = 14.4 μW cm^{-2}	3 × 3	2.5 Hz	This work
9	Sanchezia	Contact-separation mode & Handmade	Ecoflex (silicone elastomer film)	V_{oc} = 42.6 V I_{sc} = 11.2 μA p = 477.12 μW $P_{density}$ = 53 μW cm^{-2}	3 × 3	2.5 Hz	
10	Arrowhead	Contact-separation mode & Handmade	Ecoflex (silicone elastomer film)	V_{oc} = 58.7 V I_{sc} = 14.3 μA p = 839.41 μW $P_{density}$ = 93.2 μW cm^{-2}	3 × 3	2.5 Hz	
11	Banana	Contact-separation mode & Handmade	Ecoflex (silicone elastomer film)	V_{oc} = 78.5 V I_{sc} = 17.5 μA p = 1373.75 μW $P_{density}$ = 152.6 μW cm^{-2}	3 × 3	2.5 Hz	
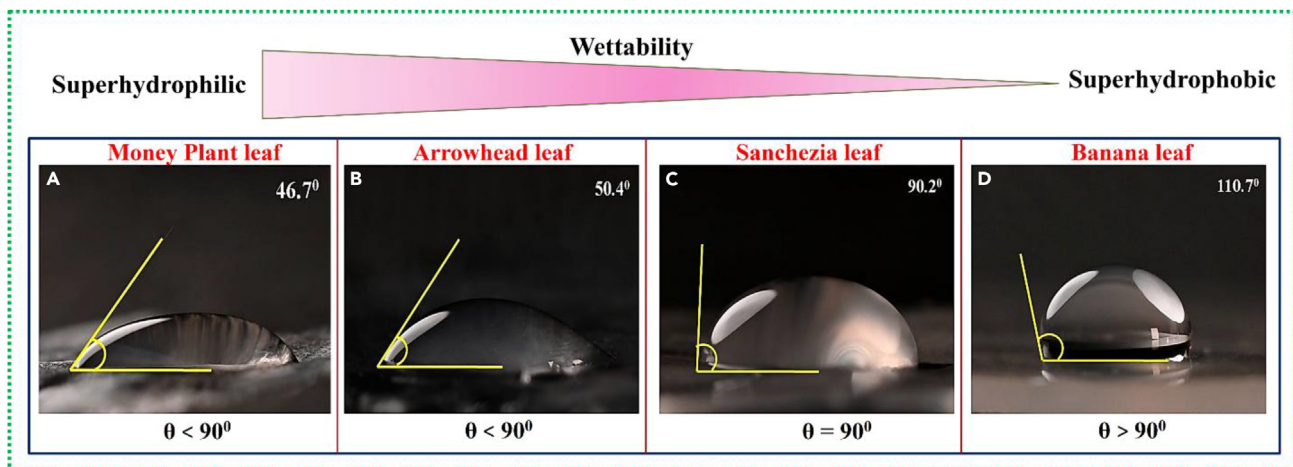
Figure 4. The different contact angles are illustrated due to the roughness of the other leaf surfaces
(A) Money Plant leaf at $\theta = 46.7°$.
(B) Arrowhead leaf at $\theta = 50.4°$.
(C) Sanchezia leaf at $\theta = 90.2°$.
(D) Banana leaf at $\theta = 110.7°$.

(2) The surface tension of the liquid (γ_{lv})
(3) The surface energy of the solid (γ_{sv})

This study used the angle of contact measurements to analyze the surface wettability of four leaf types, as shown in Figure 4: money plant, Sanchezia, arrowhead, and banana. The contact angle determines a solid surface's wettability, showing its hydrophilicity or hydrophobicity. A drop of liquid was carefully deposited on each leaf surface. The contact angle analyzer captured the droplet and analyzed the angle formed between it and the solid surface, providing information about the surface wettability of the leaf.

Surface characterization based on contact angles shows that if ($\theta < 30°$) is superhydrophilic, if ($\theta < 90°$) is hydrophilic, if ($\theta \geq 90°$) is hydrophobic, and if ($\theta > 150°$) is superhydrophobic, under these conditions, the contact angle of a money plant leaf was 46.7°, indicating that it is only moderately hydrophilic, as shown in Figure 4A. The contact angle of the Sanchezia leaf was 50.40°, showing a relatively hydrophilic surface in Figure 4B. The contact angle of the arrowhead leaf was 90.20°, indicating a slightly hydrophobic surface in Figure 4C. Finally, the contact angle of the banana leaf was 110.70°, showing a more hydrophobic surface in Figure 4D. These measurements of contact angles provided helpful information about each leaf's surface wettability. Table 2 displays the contact angle values obtained from measurements of four leaves: money plant, Sanchezia, arrowhead, and banana. These contact angle readings provide information on the wettability of each leaf's surface.

Table 2 displays the contact angle values obtained from measurements of four leaves: money plant, Sanchezia, arrowhead, and banana. These contact angle readings provide information on the wettability of each leaf's surface.

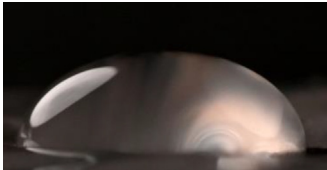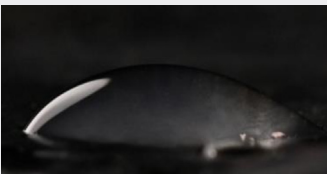## Water collection from fog using leaves

Pure drinking water is in short supply in dry and desert areas, posing a severe problem for the local population.[50] One possible solution to this issue is harvesting water from fog.[51,52] Several research groups have developed a variety of substrates with high water harvesting efficiency, but a material with high reusability and flexibility is still needed. To understand the role of surface roughness in water collection, four leaves with various surface roughnesses were used for fog harvesting.

Water was collected from a fog in four stages: (1) coalescence, (2) sliding, (3) vapor condensation, and (4) water droplet development.[53] Wenzel's equation suggests that the rougher a surface is, the better its wettability.

$$\cos \theta_m = r\cos\theta_\gamma \tag{Equation 2}$$

In this Equation, θ_γ represents the intrinsic Young's contact angle, r represents the surface roughness, and θ_m represents the observed contact angle. According to Equation 2, increasing the roughness of a surface increases its hydrophobicity. Increasing the roughness makes a hydrophilic surface more hydrophilic and a hydrophobic surface more. Using leaves to collect water from Fog is an innovative and environmentally friendly way to use the natural qualities of sure leaves to get water from foggy places. This technique is especially effective in areas with limited access to clean water, such as dry or hilly regions. Surface wettability greatly influences water collection efficiency, as discovered. Hydrophilic surfaces attract water, whereas hydrophobic surfaces resist it. Hence, leaves from four plants—money plant, Sanchezia, arrowhead, and banana—were arranged to study fog harvesting Figure 5.

Table 2. Different situations occur based on the wetting angle

S No	Leaf names	Water drop shapes	Hydrophilic/Hydrophobic	Contact angle (θ)	Wetting/Non-wetting
1	Banana		Hydrophobic	θ = 110.70 (please keep degree 110.7^0)	Non-wetting
2	Arrowhead		Hydrophobic	θ = 90.20 (please keep degree 90.2^0)	High wetting
3	Sanchezia		Hydrophilic	θ < 50.40 (please keep degree 50.4^0)	low wetting
4	Money Plant		Hydrophilic	θ < 46.70 (please keep degree 46.7^0)	Very low wetting

A commercial humidifier produces a fog stream as part of the fog collection device's design, as shown in Figure 5A. A bio-mimicking Ecoflex polymer film was placed 15 cm away from the humidifier to receive a fog stream. The polymer film angle was set vertically at 45°. The bio-inspired water collector mimics the surface qualities of leaves and other natural leaves that efficiently collect water. It is possible to question the need for artificial surfaces containing water when natural leaves may work just as well. This work also has two goals. The study demonstrates the comparable performance of manufactured surfaces to natural leaves, highlighting technological implications. Controlled studies and precise measurements are facilitated by the variability of natural leaves. While a humidifier cannot replicate natural fog conditions precisely, it offers a consistent moisture source for assessing Leaf-TENG's effectiveness under controlled conditions, overcoming the challenges associated with the complexity and unpredictability of experiments involving natural fog.

For this reason, a humidifier offers a controlled and easy method for evaluating the device's performance in humid environments. The surface's roughness, microstructures, and hydrophobicity aid in the formation and accumulation of water droplets. The water collected is measured using analytical balances set up directly under the water collector. These balances accurately measure collected water to quantify water harvesting efficiency. An electronic precision balance produced an analytical balance for measuring the collected water.

The relationship between fog and the surface was studied at two angles: 45° and 0°. At 0°, gravity is the dominant force, and the surface's wettability does not affect the interaction between the fog and the surface. Fog and surface do not interact at 90°. Therefore, to capture the middle ground in which fog and surfaces communicate, a 45° angle was chosen. The study also showed that insects prefer level surfaces with a 45° inclination angle because they elevate their backs to align with the fog flow. The researchers also investigated a 0° inclination angle to compare the results. In addition, Figures S7A—S7F shows the voltage and current output measured for polymer film angles of 30°, 45°, and 60°.

Figure 5B depicts the equipment used to gather fog water in real-time, demonstrating the system's practical application. Figure 5C shows the internal structure of the fog water collection box. Within this box, the hydrophilic and hydrophobic properties of the surfaces of leaves used for fog water collection can vary. These distinctive characteristics help leaves absorb fog water efficiently. The vapor released by the humidifier condenses into an abundance of tiny water droplets upon making contact with the rough surfaces of the leaves. These drops stick to the leaf's rough and wrinkled surfaces, making gathering and joining easier for the droplets. Therefore, larger water molecules form on the

Figure 5. Water collection from fog

Figure360▷ For a Figure360 author presentation of Figure 5, see https://doi.org/10.1016/j.isci.2024.108878.
(A) The device setup for collecting fog water.
(B) The equipment collects fog water in real-time.
(C) Inside of the fog water collection box.

surfaces of the leaves. Furthermore, the surface patterns allow the droplets to flow in a specified direction, sending them on proper steps and making it easier to drop them off at the appropriate time.

Figures 6 and 6A shows the water collection by four distinct leaves. Under wet conditions, each leaf received a different amount of water (measured in grams) at different time intervals (measured in minutes). Four water samples were collected for 1 h. Within an hour, the money plant leaf gathered 3.4 (g) of water, the Sanchezia leaf gathered 5.2 (g), the arrowhead leaf gathered 6.1 (g), and the banana leaf picked 6.9 (g). It indicates that, among the four leaves, the banana leaf collected the most water. Each leaf's humidity rises along with water accumulation. It means the area's humidity increased as the leaves gathered more water.

In addition, the researcher investigated the variation in water collection efficacy as a function of the relative intention of roughnesses facing a fog stream. Figure 6B shows that the study evaluated the water-gathering efficiency of horizontal and vertical samples. The horizontally placed samples collected a certain amount of water for an hour. On the other hand, the vertically aligned samples collected water differently than the horizontal samples. The study measured water collection by both types of samples.

Table 3 shows the initial droplet formation and movement time, elucidated on various four-leaf roughness samples. The results explained that the banana leaf roughness sample was quicker out of four leaves than those placed on the other samples. In a banana leaf, which was placed vertically, droplets formed and moved to know the roughness and the rough shape of the leaf. The fact that the banana roughness sample was hydrophobically made it easier for droplets. Changing the wettability behavior of the leaves' different roughnesses allows us to modify the amount of water collected. Initially, the banana leaf was flexible, with soft surfaces and rough leaves, and it managed water gathering. The study focuses on surface wettability, leaf morphology, and relative roughness to collect fog water. The experiment's outcome revealed authentic and valuable result (or) information for designing efficient fog water harvesting strategies, showing potential for locations with limited freshwater resources.

Fabrication of Leaf-TENG device

Due to environmental concerns, researchers are finding new ways to reuse and recycle plastic. This work used old plastic boxes to make the Leaf-TENG device in this work, as shown in Figure 7. The smooth and flat surface of the box was divided into two pieces, each measuring (7 × 3 cm). Two aluminum electrodes (2 × 1.5 cm) were attached to both sides of the plastic sheet substrate. A similar-sized Ecoflex sheet with a leaf pattern was placed under the aluminum electrode on one side of the device. After that, copper wires were attached to the electrodes for electrical connections, and both layers were securely attached on both sides, forming a Leaf-TENG device.

In recent years, 3D printing has revolutionized manufacturing by simplifying complicated and customized things. This study provides a 3D printing framework for a functional box with Leaf-TENG sensors and an LCD, as shown in Figures 8 and 8A. Figures 8B and 8C show the box's height and width dimensions. Two fabricated Leaf-TENG sensors were placed on the box to increase its use Figure 8D. When pressure is applied to these sensors to detect and convert mechanical force into electrical energy, demonstrating its touch-sensing capability, the box can be integrated with an LCD Figure 8E. A 3D-printed box protects the Leaf-TENG sensors, whether they are damaged, and LCD shields to ensure their safety and longevity. This design provides solid structural support and keeps the components securely in place.

Working principle

TENGs use the electrostatic induction and triboelectric effect to convert mechanical energy into electrical energy, as shown in Figures 9 and 9A. TENG efficacy depends on various aspects, including charge density.

Figures 9B–9E show the charge transfer mechanism between the TENG device's layers by analyzing the Leaf-TENG device's vertical contact-separation mode stages. In the TENG configuration, aluminum electrodes are the positive layers, while Ecoflex is the active negative layer. When the Ecoflex film and electrodes first come into contact Figure 9B, no potential difference exists between them. However, when a specific pressure is applied, a potential difference develops between the layers, causing separation. This potential difference allows
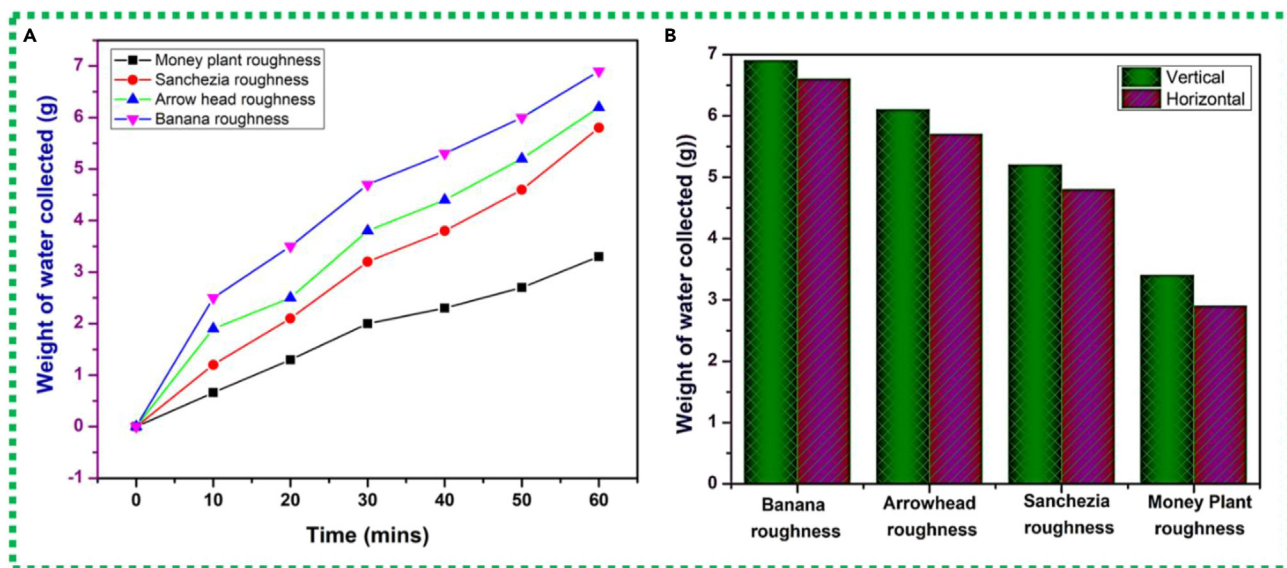
Figure 6. Comparative water collection on samples of leaf roughness
(A) Variation in water collection using different leaf roughness samples of dimensions 60 mm × 20 mm for 1 h.
(B) Water was gathered over 1 h using horizontally and vertically aligned samples.

electrons to travel from the Ecoflex layer, which has a higher affinity for electrons, to the aluminum electrode layer through an external circuit Figure 9C. Next, the system reaches an equilibrium state, and current flows from the external circuit to the ground, contributing to the positive AC signal cycle Figure 9D. Similarly, when the device gets compressed, and the contact material moves toward the Ecoflex layer, electrons are inducted and travel in the opposite direction, corresponding to the negative cycle of the AC signal Figure 9E. The maximum output value has been reached.

A COMSOL Multiphysics simulation study investigated the potential material distribution in contact-separation triboelectric nanogenerators in Figure 10. Ecoflex was used to construct the Leaf-TENG device, and the material separation distance (y1) served as the variable parameter. Set the maximum y1 range to 8 mm. The study evaluated the potential distribution on Ecoflex surfaces for y1 = 0.5 mm, 2 mm, 6 mm, and 8 mm, as shown in Figure 10A. The simulation analysis indicated that the TENG device produced a short circuit transfer charge of 4.0×10^{-10} C and a maximum potential difference of 325 V when the Ecoflex polymer and aluminum were 8 mm apart Figure 10B. These results provide essential details regarding the performance of TENGs, which may aid in developing more effective and efficient energy-harvesting systems.

Performance analysis

It evaluated the performance of the Leaf-TENG device in this study to determine its stability, electrical power density, and ability to charge capacitors in Figure 11. Figure 11A shows the criteria for selecting the Ecoflex leaf roughnesses and aluminum leaf-TENG samples that would undergo further evaluation.

Figures 11B and 11C show the open-circuit voltage and short-circuit current being measured with a digital storage oscilloscope (KEYSIGHT InfiniiVision DSOX2012A) and a Keithley Picoammeter (6485) to evaluate the device's efficiency. When the applied force 9N to

Table 3. Time taken for initial droplet formation and movement on various 4-leaf roughness samples

| S No	Four different leaves	Hydrophilic/ hydrophobic	Alignment (vertical/horizontal)	Weight of water (g)	Time is taken for initial droplet nucleation and sliding (mins)
1	Money Plant	Hydrophilic	Vertical	3.4	70
			Horizontal	2.9	63
2	Sanchezia	Hydrophilic	Vertical	5.2	55
			Horizontal	4.8	48
3	Arrowhead	Hydrophobic	Vertical	6.1	42
			Horizontal	5.7	39
4	Banana	Hydrophobic	Vertical	6.9	35
			Horizontal	6.6	20
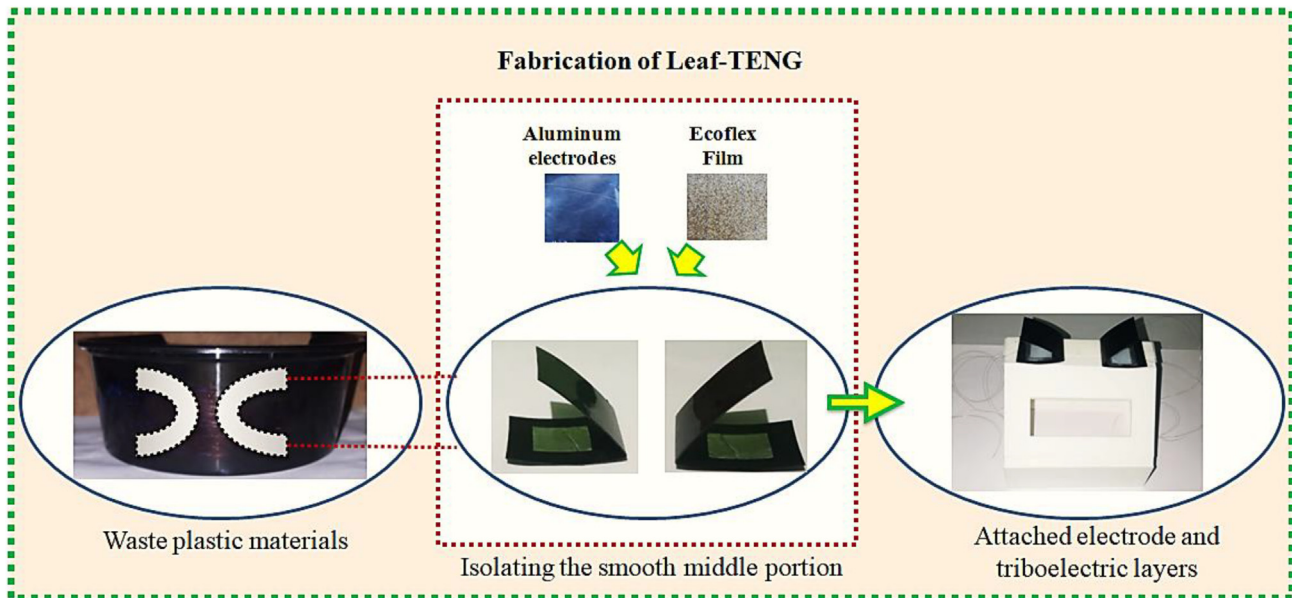
Figure 7. Step-by-step fabrication of the Leaf-TENG device made from plastic waste

the Leaf-TENG was observed, an increase in the short-circuit current and the open-circuit voltage. Different Ecoflex leaf samples were tested, like those from the money plant, Sanchezia, arrowhead, and banana. According to the results, the open-circuit voltages and currents were 17.3 V, 42.6 V, 58.7 V, and 78.5 V, and 7.5 µA, 11.2 µA, 14.3 µA, and 17.5 µA, respectively. Leaf-TENG was connected to a DF06G bridge rectifier IC and a 10 µF parallel capacitor to verify the performance of the capacitor charging technique. The Leaf-TENG's capacitor stayed fully charged for 2 min and 10 s before discharging. The charged capacitor can be a steady DC power source for small electronic devices. Figures 11D and 11E demonstrate that the rectified output appears as the capacitor charges.

A further evaluation of the device's performance involved a load analysis to determine the Leaf-TENG generated power density. This study measured the output current and voltage for a range of load resistances from 1 MΩ to 120 MΩ. As resistance increased, the current decreased from 17.5 µA to 0 µA, and the voltage increased from 0 V to 78.5 V Figure 11F. The researcher calculated the instantaneous power of the Leaf-TENG using the Equation $P = VI$ for various load resistances. The instantaneous power density was determined by dividing the instantaneous power by the material's active surface area (5 cm^2). The Leaf-TENG produced a maximum power of 58.5 µW and a power density of 2.43 µW/cm^2 at a load resistance of 65 MΩ Figure 11G, indicating that this resistance is the best for the device. It took measurements over 500 cycles a day to test the device's. stability in those ten-cycle data collection intervals and force. Figure 11H shows that the Leaf-TENG has a stable and long-lasting electricity output, with a daily output voltage of about 55 V. A comparative bar graph of the roughness of four leaves in this banana roughness is gives excellent output performance compared to the other three leaves shown in Figure 11I. These results show the device's potential for real-time capabilities.

Applications

Leaf-TENG's effectiveness was proven by showing two real-time applications: (1) as energy harvesters to power electronic devices and (2) as an Arduino-based chess timing. The following sections provide a detailed explanation of the applications, showcasing the practicality and flexibility of Leaf-TENG in practical scenarios.

Powering small-scale electronic devices

The Leaf-TENG achieved a maximum power density of 2.43 µW/cm^2 in tests. It also demonstrated a maximum voltage of 78.5 V and a current of 17.5 µA. These results powered two small electronic devices: a Lumex display and a series-connected array of 18 LEDs. To power the Lumex displays, the Leaf-TENG was connected directly between the negative and positive terminals, as shown in Figure S3A and Video S1. The Leaf-TENG was directly related to the array's negative and positive terminals to power the serially connected LEDs in Figure S3B and Video S2. These experiments demonstrate Leaf-TENG's reliability as a power supply for tiny electronics.

Chess timer using Leaf-TENG

The Leaf-TENG device was successfully deployed as a touch sensor with the help of an Arduino-based chess timer, demonstrating its innovative skills and potential applications. Standard automatic chess timers require external power sources, but the Leaf-TENG touch sensors generate electricity based on applied force in Figure 12.
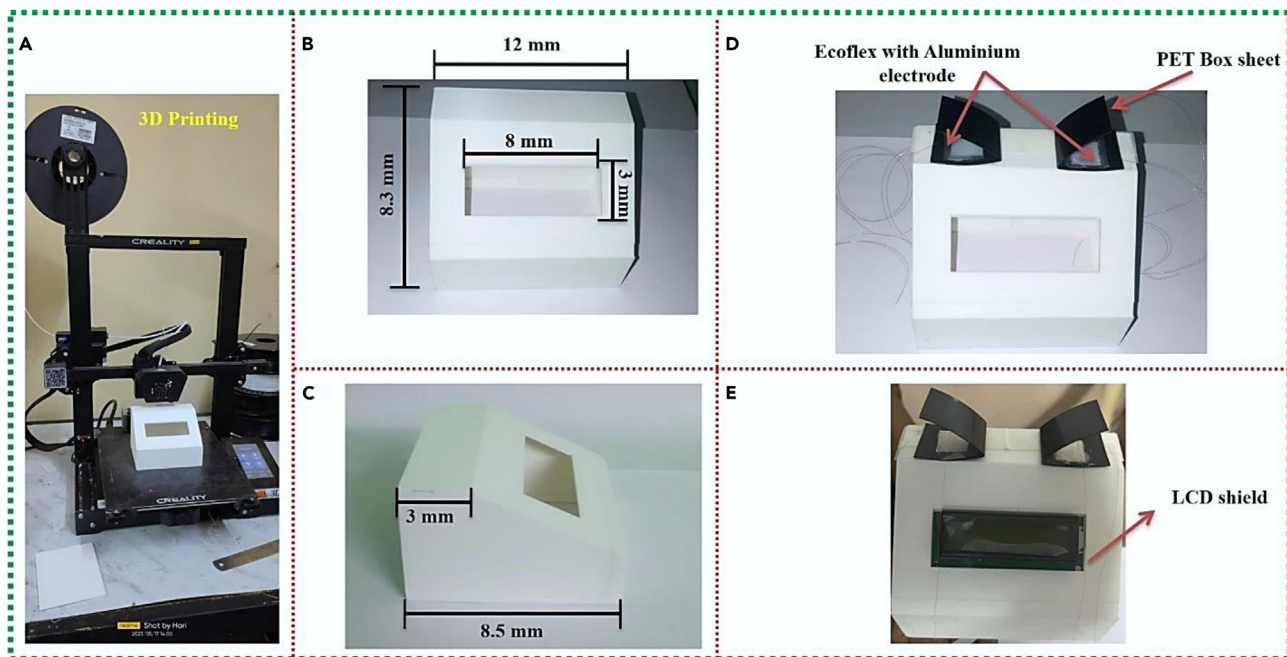
Figure 8. Integrate leaf film sensors onto the 3D printed box for chess timer application
(A) The 3D printing procedure.
(B and C) Dimensions of 3D printed boxes.
(D) Two Leaf-TENG sensors were placed on the box.
(E) LCD shield placed into the box.

A sustainable and user-friendly chess timer system was created using Leaf-TENG sensors, an Arduino Uno microcontroller board, and a 16x2 LCD shield, as shown in Figures 12A, 12B, and Video S3. The Arduino board serves as the control unit, receiving inputs from the Leaf-TENG sensors. A chess clock keeps track of the time each player has to make their moves during a regular chess game. The movement of chess pieces has no direct impact on the clock. Instead, timers for each player run down automatically. The display module shows the
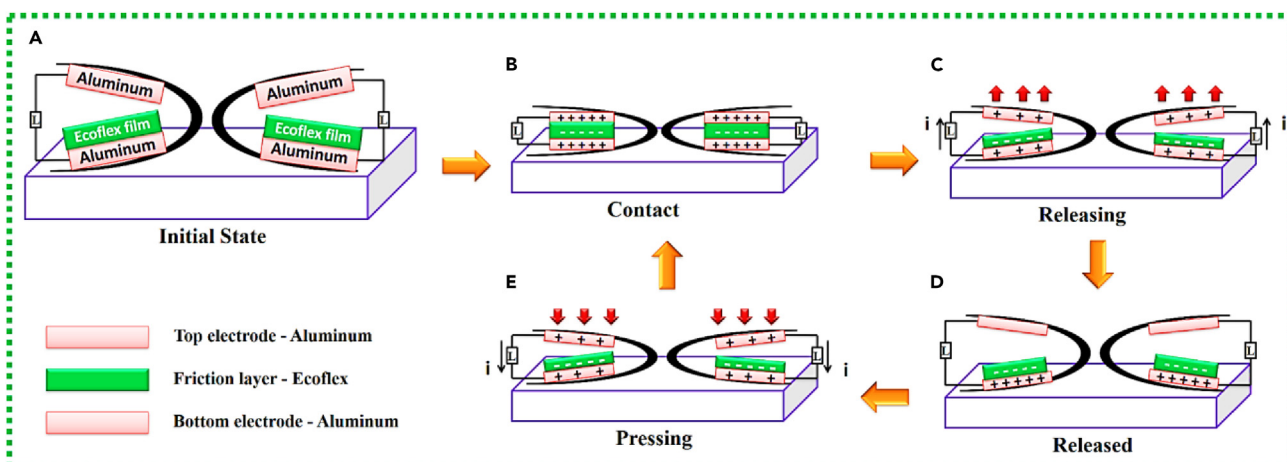

Figure 9. Working mechanism of the separation and contact mode triboelectric nanogenerator
(A) Initial.
(B) Contact.
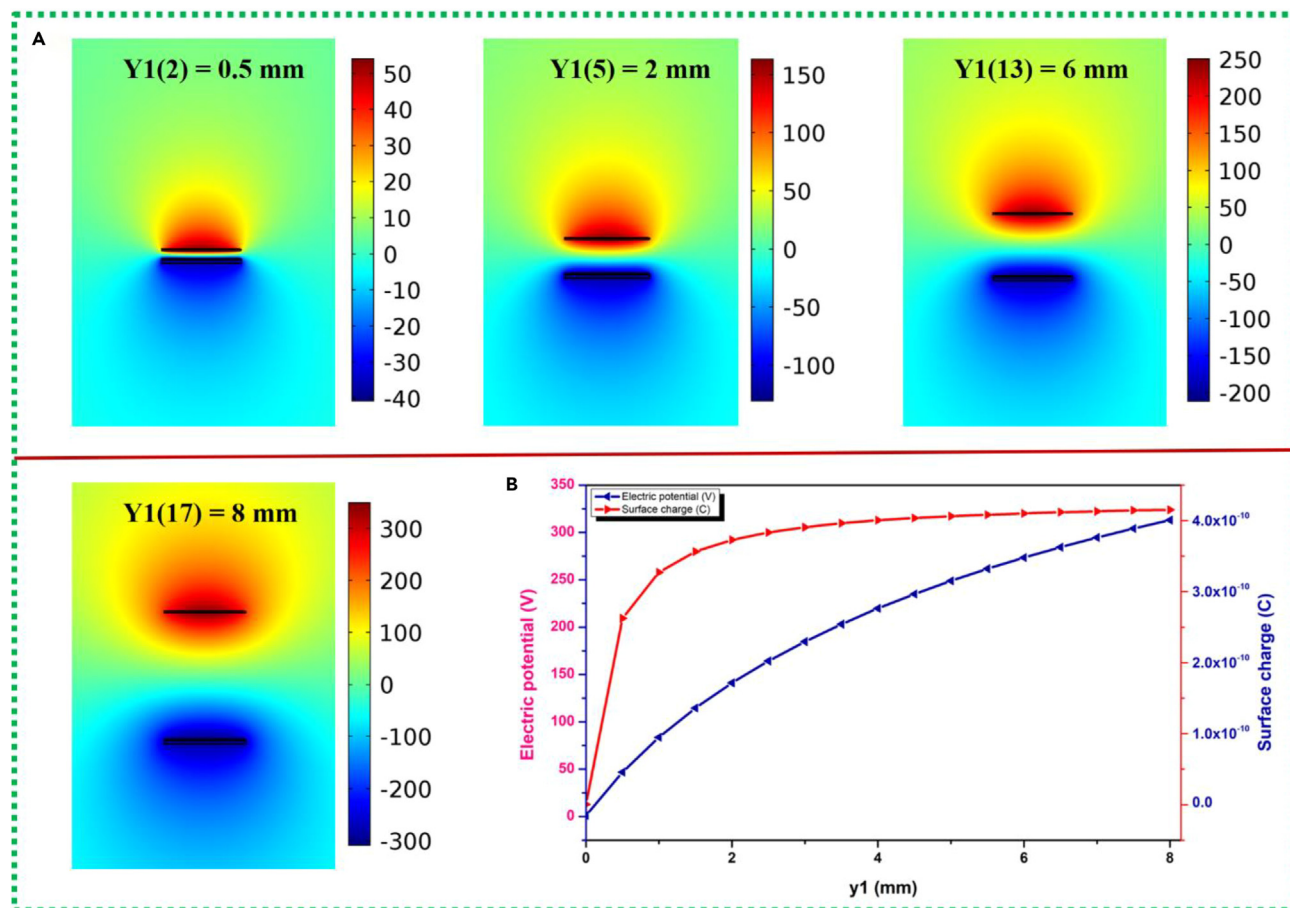(C) Releasing.
(D) Fully released.
(E) Pressing states.

Figure 10. Analysis of COMSOL simulations
(A) Y1 = 0.5 mm, Y1 = 2 mm, Y1 = 6 mm, and Y1 = 8 mm surface electrical potentials.
(B) Surface charge and electrical potential change with y1.

remaining time for each player, while the sensors detect how long each player spends on their moves. It is a standard function of every professional chess clock. The clock continues to tick regardless of where the chess pieces go. Leaf-TENG sensors can be used instead of conventional push-button switches to respond to touch inputs and take the desired action. This device also has an accurate player time tracker, minimal power consumption due to these sensors, and real-time display updates based on chess coin movements. This effective implementation demonstrates the flexibility of TENGs and their potential in various applications, such as environmental sensors, wearable electronics, and Internet of Things devices. TENGs provide a sustainable power source by absorbing mechanical energy from the environment, leading to a brighter future. The combination of novel materials and open-source electronics shows the capability of generating practical electrical advances and propelling improvements in electronics.

Leaf-TENG as a rain energy harvester

In addition, this research investigates the creation of TENG devices for rain-sensing applications. To accomplish this, the researcher used soft lithography methods and plant-shaped molds to put different designs on the surface of an Ecoflex polymer material. The study analyzes Leaf-TENG devices with these surface patterns by employing two distinct modes of operation: the freestanding triboelectric layer mode and the single electrode mode. Leaf-TENG devices detect rain in single electrode mode by detecting triboelectric charge changes when droplets hit surface patterns as shown in Figure 13. The freestanding triboelectric layer mode compares Leaf-TENG rain sensors with different surface patterns using many layers of triboelectric materials as shown in Figure 14.

Figure 13A shows the arrangement for the single electrode mode. The researcher used Ecoflex film with different leaf patterns and affixed it to an aluminum electrode to build the device. This setup showed Leaf-TENG's rain-sensing ability. Figure 13B shows that water was poured across the surface of the device to simulate rainfall. When the rainwater hit the surface with the leaf design, it started a triboelectric effect, triggering an electrical signal to be created. This signal was then collected and presented on a digital storage oscilloscope. The findings in Figures S4A and S4B demonstrate a single electrode mode mechanism device and increasing open circuit voltage with applied force
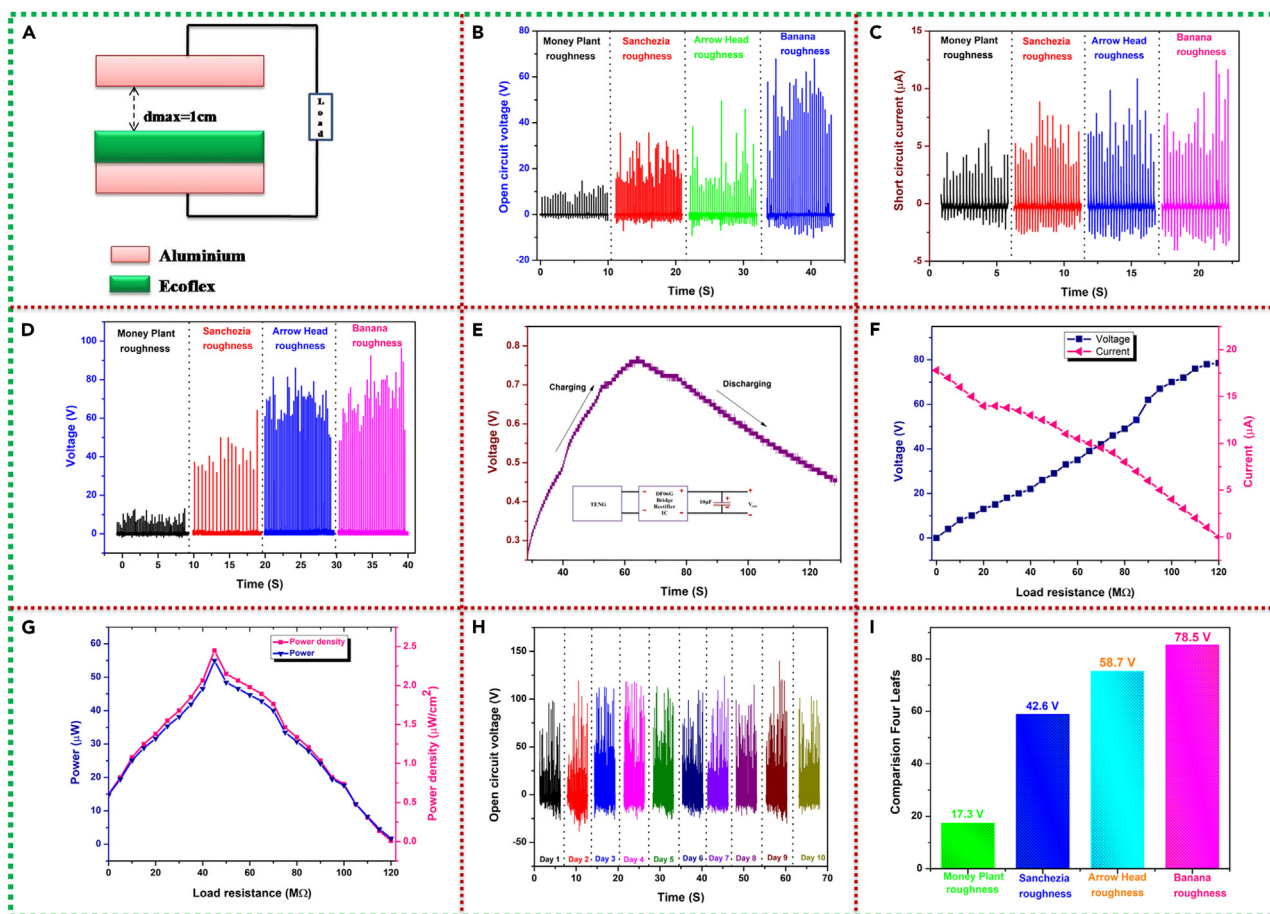
Figure 11. Leaf-TENG electrical response analysis

(A) Leaf-TENG device is the best material arrangement.

(B) The open circuit voltage corresponds to the applied force.

(C) The short-circuit current versus applied forces.

(D) Rectified output.

(E) Capacitor charging and discharging.

(F) Load analysis: variation of current and voltage to load resistances.

(G) Variation of power density and power according to load resistances.

(H) Test of Leaf-TENG stability for ten consecutive days.

(I) A bar graph comparing the characteristics of four different types of leaves.

9N continued for all four leaf roughnesses: money plant, Sanchezia, arrowhead, and banana. Among these four leaf roughnesses, the banana was provided with a high voltage of 30.2 V, and Figure 13C shows the device's rectified output performance. Rectification is essential in DC power applications like charging batteries and powering electronics. The rectification process stabilizes the DC signal that the Leaf-TENG devices generate, allowing for more efficient energy transfer and use.

Furthermore, the same single-electrode mode procedure can be extended to freestanding triboelectric layer mode. In this case, Ecoflex film with four different leaf roughnesses was placed between two aluminum electrodes to create the TENG device Figure 14A. Figure 14B shows the two electrode modes in the real-time image. In contrast, Figure S5A and S5B demonstrate the freestanding triboelectric layer mechanism device. The increasing open circuit voltage with applied force 9N continued for all four leaf roughnesses: money plant, Sanchezia, arrowhead, and banana. Among these four leaf roughnesses, the banana was provided with a high voltage of 29.3 V, and Figure 14C depicts the rectified output performance of the device.

The banana roughness Leaf-TENG device has the highest voltage output of the four leaf roughnesses tested. It shows that banana leaf surface properties boost triboelectric performance and voltage generation. The different surface patterns of the Leaf-TENG devices are then looked at for rain-sensing applications, especially in the freestanding triboelectric layer and single electrode modes. This study aims to learn whether the surface patterns influence the efficiency of the TENG devices as rain detectors.
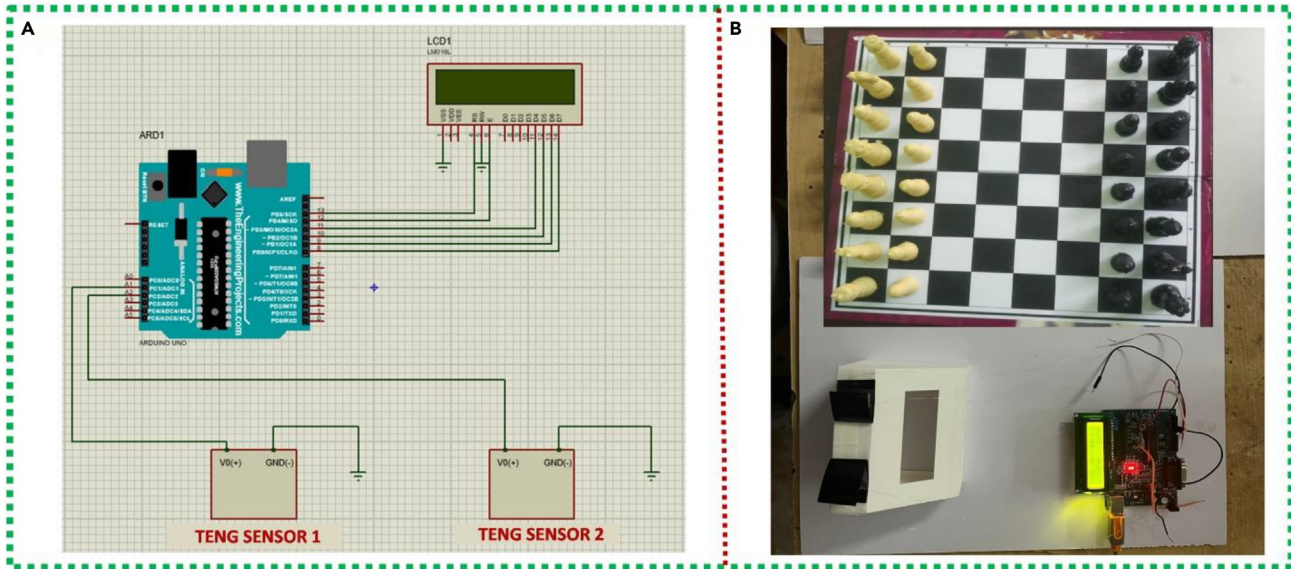
Figure 12. Real-time application of Leaf-TENG
(A) Schematic capture of an Arduino chess timer incorporating Leaf-TENG sensors.
(B) Real-time applications of Leaf-TENG technology.

The circuit diagram for connecting a Leaf-TENG sensor to a NodeMCU is shown in Figures 15 and 15A. The main parts of the setup are the NodeMCU, a signal processing module, and a Leaf-TENG sensor that was built. NodeMCU is the microcontroller, offering processing power and necessary networking features. It is the framework's controlling device, receiving and processing data from the signal processing module and the Leaf-TENG sensor. The signal processing module receives the data from the Leaf-TENG sensor and processes it. It can send out both analog and digital data at the same time. The module has four pins, two of which are for power (VCC and GND), and the other two can send analog and digital data simultaneously. The constructed Leaf-TENG sensor, a triboelectric nanogenerator, is incorporated into the circuit to utilize the triboelectric effect of mechanical movement, particularly raindrop contact. It transforms the mechanical energy of rainfall into electrical power. Figure 15B shows the actual time image. During the procedure, drops of water were deposited onto the Leaf-TENG sensor, prompting electrical signal generation. The signal processing module was in charge of receiving and processing these signals. The serial monitor displays the raindrop sensor's analysis of the collected data. The system can provide an output analysis that differentiates between various rainfall intensities by analyzing the sensor data. For example, if the raindrop activity is solid and continuous, the output is heavy rain. The sensor detects no raindrops and displays a no rain indicator on the Leaf-TENG sensor output, as shown in Video S4.
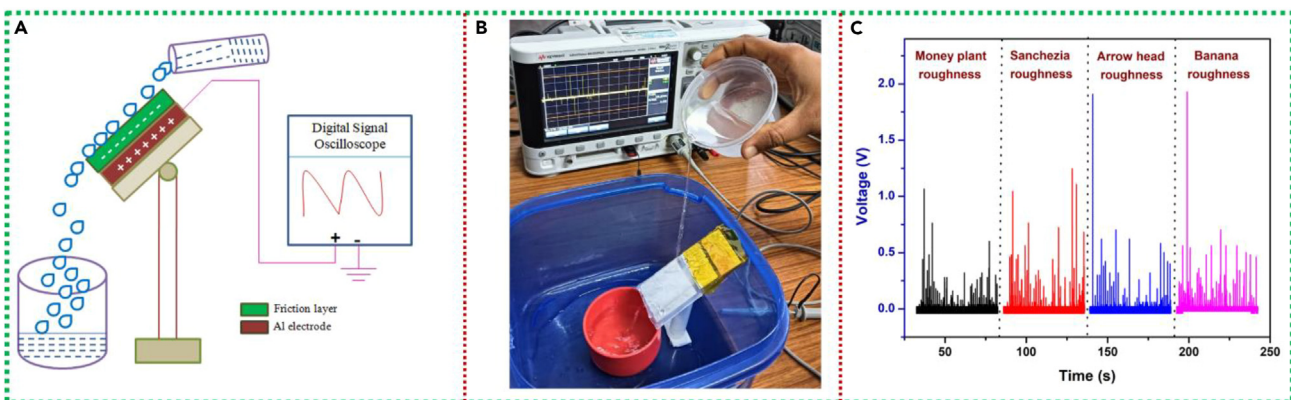

Figure 13. Leaf-TENG harvests rain energy using a single-electrode mode
(A) Leaf-TENG rain energy harvester experiment using a single electrode mode.
(B) Simulated rainfall on the device.
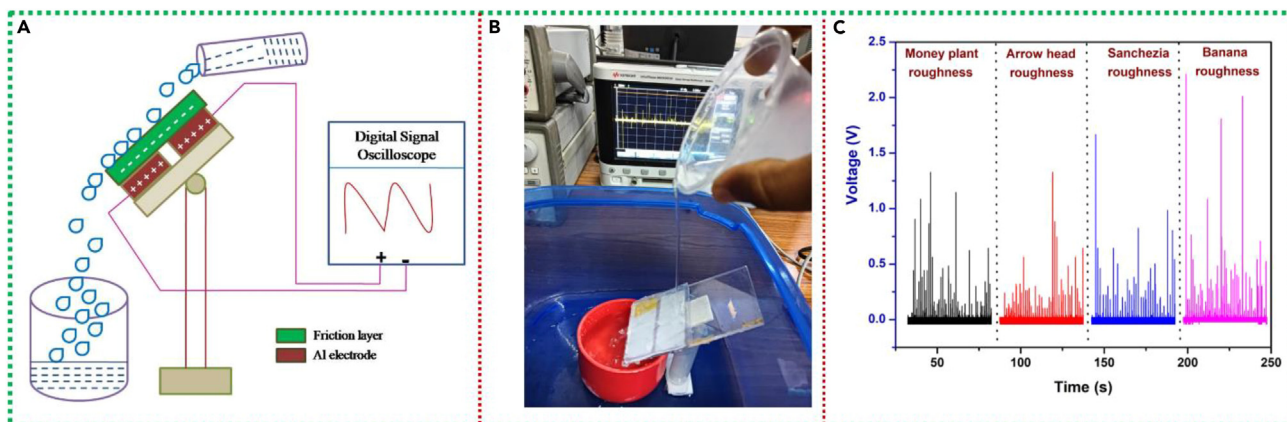(C) Rectified output voltage.

Figure 14. Leaf-TENG harvests rain energy using a freestanding triboelectric layer mode
(A) Leaf-TENG, rain-sensing experiment, using a freestanding triboelectric layer mode.
(B) Simulated rainfall on the device.
(C) Rectified output voltage.

This arrangement allows real-time monitoring and analysis of rainfall data from the Leaf-TENG sensor, revealing rainfall intensity. The Leaf-TENG sensor can precisely identify rainfall occurrences based on variations in electrical output from droplets touching the leaf surface. Rainfall may be monitored in real-time using this information. It can be built into irrigation systems to give instantaneous updates on soil moisture. The irrigation system can save water resources by delaying or reducing watering when rainfall is detected. During testing, the Leaf-TENG reached up to 30 V. These findings powered two tiny electrical devices: a Lumex display and a 25-LED series-connected array. As shown in Figure S6A and Video S5, the Leaf-TENG was connected directly between the negative and positive terminals to supply power to the Lumex displays. Figure S6B and Video S6 show that the Leaf-TENG was directly linked to the positive and negative terminals of the array to power the LEDs that were connected in series. These tests show Leaf-TENG's power supply durability for tiny circuits.

Conclusions

Our study concluded that it successfully introduced the soft lithography technique using four different leaf surfaces and thoroughly evaluated and analyzed the surface morphology of the polymer films obtained with goniometric drop morphology and a 3D optical profilometer. The efficiency of the films was validated through experiments performed on chess timing systems, showcasing their potential as touch-sensitive switches in real-world applications for harvesting biomechanical energy. The Leaf-TENG was experimentally evaluated using four distinct Ecoflex leaf roughnesses. Compared to the other three-leaf roughnesses, the banana roughness performed best, with greater short-circuit current (I_{sc}) and open-circuit voltage (V_{oc}) values of 17.5 μA and 78.5 V, respectively. Also, when combined with leaf-patterned films, the Leaf-TENG achieved an incredible power density of 2.43 μW/cm^2 during harvesting. Furthermore, integrated with the leaf-patterned films, the fabricated triboelectric nanogenerator demonstrated promising capabilities as a self-powered rain sensor for fog water collection. These findings contribute valuable insights into energy harvesting and present a sustainable and cost-effective approach for addressing water
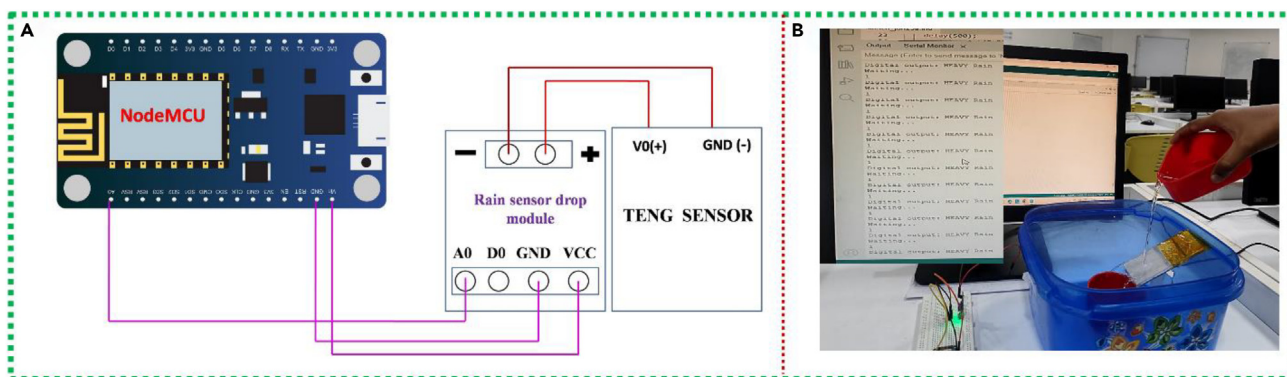

Figure 15. Rain sensor for Leaf-TENG
(A) The circuit diagram for interfacing a Leaf-TENG sensor to NodeMCU.
(B) Leaf-TENG sensor water droplet deposition in real-time.

scarcity issues in dry regions. Our work will lead to more research and development in the field, which will help make the future more sustainable and greener.

Limitations of the study

The study of leaf roughnesses and their performance was done in a lab, which may limit its applicability to real-world situations where environmental influences could affect performance. Also, whereas the Leaf-TENG showed potential for harvesting energy, its ability to be scaled up and its long-term power in outdoor environments require further examination. Furthermore, evaluating the constructed triboelectric nanogenerator as a rain sensor was limited to collecting fog water. As a result, further field research was required to confirm its effectiveness in various weather conditions and collection scenarios. These limitations emphasize the necessity for extensive field trials and durability testing to determine these technology's feasibility and reliability in different environments.

STAR★METHODS

Detailed methods are provided in the online version of this paper and include the following:

- KEY RESOURCES TABLE
- RESOURCE AVAILABILITY
  - Lead contact
  - Materials availability
  - Data and code availability
- METHOD DETAILS

SUPPLEMENTAL INFORMATION

Supplemental information can be found online at https://doi.org/10.1016/j.isci.2024.108878.

AUTHOR CONTRIBUTIONS

S.R.B.: Conceptualization, Data curation, Formal analysis, Investigation, Methodology, Software, Validation, Visualization, Writing – original draft, Writing – review and editing. A.C.: Data curation, Investigation, Methodology, Resources, Writing – original draft, Writing – review and editing.

DECLARATION OF INTERESTS

There is no conflict of interest to declare.

REFERENCES

1. Shah, A.V., Schade, H., Vanecek, M., Meier, J., Vallat-Sauvain, E., Wyrsch, N., Kroll, U., Droz, C., and Bailat, J. (2004). Thin-film silicon solar cell technology. Progress in Photovoltaics. 12, 113–142.

2. Wang, J., Wu, C., Dai, Y., Zhao, Z., Wang, A., Zhang, T., and Wang, Z.L. (2017). Achieving ultrahigh triboelectric charge density for efficient energy harvesting. Nat. Commun. 8, 88–97.

3. Lin, Z., Chen, J., and Yang, J. (2016). Recent Progress in Triboelectric Nanogenerators as a Renewable and Sustainable Power Source. J. Nanomater. 2016, 1–24.

4. Begum, S.R., and Chandrasekhar, A. (2023). Opportunities and Challenges in Power Management Systems for Triboelectric Nanogenerators. ACS Appl. Electron. Mater. 5, 1347–1375.

5. Lin, Z.H., Cheng, G., Lin, L., Lee, S., and Wang, Z.L. (2013). Water-solid surface contact electrification and its use for harvesting liquid-wave energy. Angew. Chem., Int. Ed. Engl. 52, 12545–12549.

6. Wang, S., He, M., Weng, B., Gan, L., Zhao, Y., Li, N., and Xie, Y. (2018). Stretchable and wearable triboelectric nanogenerator based on kinesio tape for self-powered human motion sensing. Nanomaterials 8, 657.

7. Wang, S., Wang, X., Wang, Z.L., and Yang, Y. (2016). Efficient Scavenging of Solar and Wind Energies in a Smart City. ACS Nano 10, 5696–5700.

8. Cao, X., Jie, Y., Wang, N., and Wang, Z.L. (2016). Triboelectric Nanogenerators Driven Self-Powered Electrochemical Processes for

Energy and Environmental Science. Adv. Energy Mater. 6.

9. Ravichandran, A.N., Depoutot, F., Kharbouche, E., Hamand, M., Ramuz, M., and Blayac, S. (2021). Demonstration of friction-based triboelectric nanogenerator and integration in a power-balanced fully autonomous system. Nano Energy 83, 105796.

10. Yi, F., Lin, L., Niu, S., Yang, P.K., Wang, Z., Chen, J., Zhou, Y., Zi, Y., Wang, J., Liao, Q., et al. (2015). Stretchable-rubber-based triboelectric nanogenerator and its application as self-powered body motion sensors. Adv. Funct. Mater. 25, 3688–3696.

11. Braendlein, M., Lonjaret, T., Leleux, P., Badier, J.M., and Malliaras, G.G. (2017). Voltage Amplifier Based on Organic Electrochemical Transistor. Adv. Sci. 4, 1600247.

12. Song, W., Gan, B., Jiang, T., Zhang, Y., Yu, A., Yuan, H., Chen, N., Sun, C., and Wang, Z.L. (2016). Nanopillar Arrayed Triboelectric Nanogenerator as a Self-Powered Sensitive Sensor for a Sleep Monitoring System. ACS Nano 10, 8097–8103.

13. Khandelwal, G., Minocha, T., Yadav, S.K., Chandrasekhar, A., Maria Joseph Raj, N.P., Gupta, S.C., and Kim, S.J. (2019). All edible materials derived biocompatible and biodegradable triboelectric nanogenerator. Nano Energy 65, 104016.

14. Zhang, Y., Zhou, Q., Zhu, J., Yan, Q., Dou, S.X., and Sun, W. (2017). Nanostructured Metal Chalcogenides for Energy Storage and Electrocatalysis. Adv. Funct. Mater. 27.

15. Yang, Y., Xie, L., Wen, Z., Chen, C., Chen, X., Wei, A., Cheng, P., Xie, X., and Sun, X. (2018). Coaxial Triboelectric Nanogenerator and Supercapacitor Fiber-Based Self-Charging Power Fabric. ACS Appl. Mater. Interfaces 10, 42356–42362.

16. Yar, A., Kinas, Z., Karabiber, A., Ozen, A., Okbaz, A., and Ozel, F. (2021). Enhanced performance of triboelectric nanogenerator based on polyamide-silver antimony sulfide nanofibers for energy harvesting. Renew. Energy 179, 1781–1792.

17. Wang, Y., Yang, Y., and Wang, Z.L. (2017). Triboelectric Nanogenerators as Flexible Power Sources at Nature Research.

18. Zhang, R., and Olin, H. (2020). Material choices for triboelectric nanogenerators: A critical review. EcoMat 2, 1–13.

19. Yang, H., Fan, F.R., Xi, Y., and Wu, W. (2021). Design and engineering of high-performance triboelectric nanogenerator for ubiquitous unattended devices. EcoMat 3, 1–36.

20. Wang, X., Niu, S., Yi, F., Yin, Y., Hao, C., Dai, K., Zhang, Y., You, Z., and Wang, Z.L. (2017). Harvesting Ambient Vibration Energy over a Wide Frequency Range for Self-Powered Electronics. ACS Nano 11, 1728–1735.

21. Baik, J.M., and Lee, J.P. (2019). Strategies for ultrahigh outputs generation in triboelectric energy harvesting technologies: from fundamentals to devices. Sci. Technol. Adv. Mater. 20, 927–936.

22. Yang, W., Wang, X., Li, H., Wu, J., Hu, Y., Li, Z., and Liu, H. (2019). Fundamental research on the effective contact area of micro-/nano-textured surface in triboelectric nanogenerator. Nano Energy 57, 41–47.

23. Wu, J., Zheng, Y., and Li, X. (2021). Recent progress in self-powered sensors based on triboelectric nanogenerators. Sensors 21, 7129.

24. Basith, S.A., and Chandrasekhar, A. (2023). COVID-19 clinical waste reuse: A triboelectric touch sensor for IoT-cloud supported smart hand sanitizer dispenser. Nano Energy 108, 108183.

25. Sun, C., Shi, Q., Hasan, D., Yazici, M.S., Zhu, M., Ma, Y., Dong, B., Liu, Y., and Lee, C. (2019). Self-powered multifunctional monitoring system using hybrid integrated triboelectric nanogenerators and piezoelectric microsensors. Nano Energy 58, 612–623.

26. Wang, N., Liu, Y., Ye, E., Li, Z., and Wang, D. (2023). Innovative Technology for Self-Powered Sensors: Triboelectric Nanogenerators. Advanced Sensor Research 2, 2200058.

27. Jin, L., Tao, J., Bao, R., Sun, L., and Pan, C. (2017). Self-powered Real-time Movement Monitoring Sensor Using Triboelectric Nanogenerator Technology. Sci. Rep. 7, 10521.

28. Wu, Z., Cheng, T., and Wang, Z.L. (2020). Self-powered sensors and systems based on nanogenerators. Sensors 20, 2925.

29. Guo, H., Yeh, M.H., Lai, Y.C., Zi, Y., Wu, C., Wen, Z., Hu, C., and Wang, Z.L. (2016). All-in-One Shape-Adaptive Self-Charging Power Package for Wearable Electronics. ACS Nano 10, 10580–10588.

30. Wen, Z., Yeh, M.H., Guo, H., Wang, J., Zi, Y., Xu, W., Deng, J., Zhu, L., Wang, X., Hu, C., et al. (2016). Self-powered textile for Wearable electronics by hybridizing fiber-shaped nanogenerators, solar cells, and supercapacitors. Sci. Adv. 2, e1600097.

31. Basith, S.A., and Chandrasekhar, A. (2023). Synergistic Effect of Dual Surface Modified Ecoflex Polymer for Dynamic Triboelectric Nanogenerator Towards Sustainable Battery-Free Tally Counter. Adv. Mater. Technol. 8, 1–15.

32. Judy, J.W. (2001). Microelectromechanical Systems (MEMS): Fabrication , Design and, p. 1115.

33. Paul, E.W., Ricco, A.J., and Wrighton, M.S. (1985). Resistance of Polyanillne Films as a Function of Electrochemical Potential and the Fabrication of Poiyanlline-Based Microelectronic Devices, pp. 1441–1447.

34. Schneider, F., Draheim, J., Kamberger, R., and Wallrabe, U. (2009). Sensors and Actuators A : Physical Process and material properties of polydimethylsiloxane. (PDMS) for Optical MEMS 151, 95–99.

35. Volpatti, L.R., and Yetisen, A.K. (2014). Commercialization of microfluidic devices. Trends Biotechnol. 32, 347–350.

36. Xia, Y., and Whitesides, G.M. Soft Lithography

37. Wang, H., Shi, H., and Wang, Y. (2015). The wetting of leaf surfaces and its ecological significances. In Wetting and Wettability, M. Aliofkhazraei, ed. (In Tech).

38. Kumar, C., Palacios, A., Surapaneni, V.A., Bold, G., Thielen, M., Licht, E., Higham, T.E., Speck, T., and Le Houérou, V. (2019). Replicating the complexity of natural surfaces: Technique validation and applications for biomimetics, ecology and evolution. Philos. Trans. A Math. Phys. Eng. Sci. 377, 20180265.

39. Sun, Y., Gao, X., Jinnong, L., and Chen, Y. (2018). Comparative Study on Wettability of Typical Plant Leaves and Biomimetic Preparation of Superhydrophobic Surface of Aluminum Alloy. 04004.

40. Senarathna, D., and Wanniarachchi, W.K.I.L. (2020). Replication of the Surface Wettability of Plant Leaves with Different Surface Morphologies Using Soft Lithography Replication of the Surface Wettability of Plant Leaves with Di ® Erent Surface Morphologies Using Soft Lithography.

41. Sue, N. (2010). Sun - Artificial Lotus Leaf by Nanocasting, pp. 1–4.

42. Lee, Y.C., Thompson, H.M., and Gaskell, P.H. (2009). Thin film flow over flexible membranes containing surface texturing: Bio-inspired solutions. In Proceedings of the Institution of Mechanical Engineers, Part J: Journal of Engineering Tribology, 223Proceedings of the Institution of Mechanical Engineers, Part J: Journal of Engineering Tribology, pp. 337–345.

43. Li, X., Wang, G., Moita, A.S., Zhang, C., Wang, S., and Liu, Y. (2020). Fabrication of bio-inspired non-fluorinated superhydrophobic surfaces with anti-icing property and its wettability transformation analysis. Appl. Surf. Sci. 505, 144386.

44. Jie, Y., Jia, X., Zou, J., Chen, Y., Wang, N., Wang, Z.L., and Cao, X. (2018). Natural Leaf Made Triboelectric Nanogenerator for Harvesting Environmental Mechanical Energy. Adv. Energy Mater. 8, 1–7.

45. Meder, F., Must, I., Sadeghi, A., Mondini, A., Filippeschi, C., Beccai, L., Mattoli, V., Pingue, P., and Mazzolai, B. (2018). Energy Conversion at the Cuticle of Living Plants. Adv. Funct. Mater. 28, 1–8.

46. Feng, Y., Zhang, L., Zheng, Y., Wang, D., Zhou, F., and Liu, W. (2019). Leaves based triboelectric nanogenerator (TENG) and TENG tree for wind energy harvesting. Nano Energy 55, 260–268.

47. Adamson, A., and Gast, A. (1997). Arthur W. Adamson, Alice P (Gast - Physical chemistry of surfaces-Wiley).

48. Young, T. (1805). An essay on the cohesion fluids. Philos. Trans. R. Soc. Lond. B Biol. Sci. 95, 65–87.

49. Vickerman, J.C., and Gilmore, I.S. (2009). Surface Analysis - the Principal Techniques, Second Edition.

50. Mekonnen, M.M., and Hoekstra, A.Y. (2016). Sustainability: Four billion people facing severe water scarcity. Sci. Adv. 2, 1–7.

51. Sharma, V., Yiannacou, K., Karjalainen, M., Lahtonen, K., Valden, M., and Sariola, V. (2019). Large-scale efficient water harvesting using bioinspired micro-patterned copper oxide nanoneedle surfaces and guided droplet transport. Nanoscale Adv. 1, 4025–4040.

52. Raj, S.S., Davis, D., Viswanathan, P., and Chandrasekhar, A. (2022). Compositionally Homogeneous Soft Wrinkles on Elastomeric Substrates : Novel Fabrication Method , Water Collection from Fog , and Triboelectric Charge Generation, pp. 1–12.

53. Ura, D.P., Knapczyk-Korczak, J., Szewczyk, P.K., Sroczyk, E.A., Busolo, T., Marzec, M.M., Bernasik, A., Kar-Narayan, S., and Stachewicz, U. (2021). Surface Potential Driven Water Harvesting from Fog. ACS Nano 15, 8848–8859.

STAR★METHODS

KEY RESOURCES TABLE

REAGENT or RESOURCE	SOURCE	IDENTIFIER
Other		
Leaves	Near home side and gardens	N/A
Ecoflex polymer (Platinum Cure Silicon Rubber)	SMOOTH-ON	Me

RESOURCE AVAILABILITY

Lead contact

Further information and requests for resources should be directed to and will be fulfilled by the lead contact, Arunkumar Chandrasekhar, arunkumar.c@vit.ac.in.

Materials availability

This study did not generate any new unique reagents.

Data and code availability

This study generates data, and the code is available at https://github.com/RuksanaECE/LeafWork.

METHOD DETAILS

All methods can be found in the accompanying https://github.com/RuksanaECE/LeafWork.